JOURNAL OF THE ROYAL SOCIETY Interface

Premature deactivation of soleus during the propulsive phase of cat jumping

Motoshi Kaya, Tim R Leonard and Walter Herzog

J. R. Soc. Interface 2008 **5**, 415-426
doi: 10.1098/rsif.2007.1158

JOURNAL OF THE ROYAL SOCIETY Interface

J. R. Soc. Interface (2008) **5**, 415–426
doi:10.1098/rsif.2007.1158
Published online 11 September 2007

Premature deactivation of soleus during the propulsive phase of cat jumping

Motoshi Kaya†, Tim R. Leonard and Walter Herzog*

Faculty of Kinesiology, Human Performance Laboratory, University of Calgary, 2500 University Drive NW, Calgary, Alberta, Canada T2N 1N4

It has been shown that cat soleus (SOL) forces remain nearly constant despite increases in electromyography (EMG) activity for increasing speeds of locomotion, while medial gastrocnemius (MG) forces and EMG activity increase in parallel. Furthermore, during jumping, average cat SOL forces decrease, while average EMG activity increases dramatically compared with walking conditions. Finally, during rapid paw-shake movements, SOL forces and EMG activities are nearly zero. Based on these results, we hypothesized that the SOL is deactivated, despite ankle extensor requirements, if the contractile conditions limit SOL force potential severely. The purposes of this study were to (i) investigate SOL EMG activity and force as a function of its contractile conditions during jumping, (ii) test whether SOL EMG activity is associated with SOL contractile conditions, and (iii) determine the functional implications of SOL EMG activity during jumping. It was found that the SOL was prematurely deactivated in two distinct phases during the propulsive phase of jumping, in which shortening speeds approached or even exceeded the maximal speed of muscle shortening. We concluded that the SOL was prematurely deactivated to save energy because its mechanical work output approached zero, and speculated that the first phase of deactivation might be caused by a decrease in group Ia firing associated with active shortening and the second by a pre-programmed response inherent to the central pattern generator.

Keywords: cat jumping; force sharing; muscle inhibition; contractile conditions

1. INTRODUCTION

Direct measurement of the cat ankle extensor forces has been the primary model to study force-sharing among synergistic muscles. It has been observed that there is a distinct difference in the division of labour between the cat medial gastrocnemius (MG) and soleus (SOL). For example, peak SOL force is nearly constant for a great range of locomotion speeds, while peak MG force increases with increasing movement demands (Walmsley *et al.* 1978; Hodgson 1983). In contrast to the predictable and expected changes in MG force and electromyography (EMG) activity, the nearly constant SOL force was thought to be caused by either a nearly constant and maximal EMG activity even at slow speeds of movement (Walmsley *et al.* 1978) or a speed-dependent inhibition through rubrospinal and cutaneous pathways (Burke *et al.* 1970), which offsets the increased excitatory input associated with increased speeds of locomotion (Hodgson 1983). For steep uphill walking, Gregor *et al.* (2001) found that SOL force decreased when compared with level walking, and suggested that the decrease in SOL force was associated with an inhibition of the SOL through MG force-dependent pathways (Nichols 1999).

There are several potential reasons why the SOL forces are not in parallel with EMG activity but are primarily associated with its contractile properties. First, the SOL is composed of slow-twitch fibres (approx. 100%; Ariano *et al.* 1973) and, second, the SOL is an essentially parallel-fibred muscle (Sacks & Roy 1982) that magnifies fibre/sarcomere shortening speed for a given muscle shortening speed compared with the unipennate-fibred MG. Finally, the SOL is a monoarticular muscle whose shortening speed is directly linked to ankle plantar flexion, while the shortening speed of the biarticular MG caused by ankle plantar flexion is partly offset by muscle stretching caused by knee extension for most locomotor conditions (Kaya *et al.* 2003). Thus, SOL forces are probably affected to a greater degree by the contractile conditions than the MG forces.

Recently, we found that SOL EMG activity increased with increasing speeds of locomotion, and for uphill when compared with level walking, while the SOL force remained nearly constant (Kaya *et al.* 2003). These results suggested that, in contrast to the published literature (Walmsley *et al.* 1978; Hodgson 1983), SOL forces are not constant owing to constant EMG activity, but despite changes in EMG activity. Rather, SOL EMG activity is regulated so that decreases in force potential, associated with changes

*Author for correspondence (walter@kin.ucalgary.ca).
†Present address: Tohoku University Biomedical Engineering Research Organization, 6-6-11-901, Aramaki, Aoba-ku, Sendai 980-8579, Japan.

Received 9 July 2007
Accepted 21 August 2007

in the contractile conditions, are offset to maintain SOL force constant during locomotor activities. Thus, one may ask how SOL activity is regulated for high-speed movements in which SOL force potential is greatly decreased owing to extreme contractile conditions (e.g. operating at short muscle/fibre length on the ascending limb of the force–length curve and/or at high muscle/fibre shortening speed on the force–velocity curve).

For the purpose of this study, we hypothesized that SOL EMG activity is associated with SOL contractile conditions for high-speed movements and, specifically, that SOL EMG activity decreases with a decrease in SOL force potential caused by high speeds of shortening (i.e. force–velocity relationship; Hill 1938). In order to test this hypothesis, we selected jumping as the experimental movement. In jumping, the SOL contractile conditions change from near-optimal length and an isometric contraction during the preparatory phase to near-maximal speeds of shortening and short muscle lengths during the propulsive phase (Smith *et al.* 1977; Walmsley *et al.* 1978; Zajac 1985). It has been observed that average SOL force is decreased substantially in jumping when compared with slow walking, despite a 50% increase in average EMG activity (Walmsley *et al.* 1978). However, Walmsley *et al.* (1978) based their results on averaged EMG activity and force across the entire jump phase, while the SOL contractile conditions changed substantially and continuously. Thus, activation/deactivation phenomena, as well as instantaneous forces as a function of the corresponding contractile conditions, could not be analysed.

The purposes of this study were to (i) investigate SOL EMG activity and force as a function of the contractile conditions during jumping, (ii) test whether SOL EMG activity is associated with SOL contractile conditions, and (iii) determine the functional implications of SOL EMG activity during jumping. For this purpose, *in vivo* muscle forces and EMG activities from cat MG and SOL were obtained, and the corresponding hindlimb kinematics and kinetics were measured for jumping movements in six cats.

2. METHOD

2.1. Cat training

Six outbred male adult cats (5.3 ± 1.2 kg) were trained to perform slow walking ($0.4\ \mathrm{m\ s^{-1}}$) on a motor-driven treadmill at $0.4\ \mathrm{m\ s^{-1}}$ ($n=23$, 43, 17, 8, 17 and 12 steps performed by six individual animals) and jumping from two force platforms onto a 60 cm high box ($n=4$, 6, 12, 2, 8 and 3 trials performed by six individual animals). Training sessions were conducted five times a week for approximately 1 hour, for a minimum of two months prior to the surgical implantation of tendon force transducers and EMG electrodes. At the end of each successful training session, rewards (food or brushing) were given.

2.2. Muscle force and EMG measurement

For measurement of MG and SOL forces, E-shaped stainless steel tendon force transducers were implanted onto the separated tendons (Walmsley *et al.* 1978). The EMG activities of these muscles and tibialis anterior (TA) were measured using indwelling, bipolar, fine wire electrodes (Herzog *et al.* 1993). All signals were transmitted by telemetry to a custom-built amplifier and stored in a PC at 2000 Hz per channel. After the implantation of the sensors, training was resumed 1 day after surgery to prevent the formation of adhesions around the ankle, and to accelerate the recovery process. Measurements were carried out when cats had completely recovered (7–10 days) from surgery based on the assessment of the ground reaction forces and resultant joint moments of the implanted hindlimb (see the Appendix A.1). All surgical procedures were performed according to the guidelines of the Canadian Council on Animal Care and were approved by the Life Sciences Animal Ethics Committee of the University of Calgary. For a more detailed description of the surgical procedures and the measurement of tendon forces and EMG activities, see Herzog *et al.* (1993).

2.3. Hindlimb kinematics and kinetics

Reflective markers (10 mm diameter spheres) were placed over the hip, knee, ankle and metatarsophalangeal (MP) joints, and the toe of the instrumented hindlimb to obtain knee, ankle and MP joint angles. The positions of these markers were recorded using a high-speed camera (200 Hz; V-14B, NAC, Inc., Tokyo, Japan) and were manually digitized using a custom-designed program written in MATLAB (Math Works, Inc., Natick, MA, USA). For synchronization of the high-speed video images with the muscle force and EMG data, a series of voltage pulses was sent to the computer simultaneously with a light-emitting diode (LED) pulse that was recorded on the video images. In order to avoid errors caused by skin marker movement, the location of the knee joint centre was calculated using an optimization procedure, in which the estimated location of the knee joint centre was optimized to be the one closest to the measured location of the knee marker, with the constraint that the distances from the estimated knee joint centre to the measured ankle and hip joints were the same as the measured shank and thigh lengths, respectively. This optimization was performed using the MATLAB function, 'fmincon' (Math Works, Inc., Natick, MA, USA).

The ground reaction forces of the instrumented hindlimb were measured using a force platform (DRMC36, AMTI, Newton, MA, USA) and stored simultaneously with the muscle forces and EMG signals in a computer at 2000 Hz per channel. The resultant joint moments at the ankle were calculated using the inverse dynamics approach (Andrews 1995) with hindlimb kinematics and ground reaction forces obtained directly, and inertial properties of body segments estimated using equations given by Hoy & Zernicke (1985). In this study, extensor moments were defined as positive.

2.4. Analyses of EMG and contractile conditions

The amplified EMG signals (gain = 700) were high-pass filtered with a cut-off frequency of 15 Hz. EMG signal

magnitude was quantified using the average root mean square (RMS) values of the full-wave rectified EMG activity between the onset and the offset of EMG activity for locomotion (Kaya *et al.* 2003) and during the defined phases for jumping (see §§2.5 and 2.6 for definition of jumping phases and deactivation phases).

Muscle-tendon lengths of the MG and SOL were calculated using the recorded joint kinematics and the tendon travel technique (Grieve *et al.* 1978). Speeds of muscle-tendon shortening were calculated as the first time derivative of the muscle-tendon length using a quintic spline function (GCVSPL; Woltring 1986) and shortening was defined as positive. The normalized shortening speeds were obtained in the following way: first, the standardized shortening speed ($\bar{V}_i$, i=MG or SOL) was obtained by dividing the speeds of MG/SOL shortening (V_i) by their optimal lengths (L_i^{opt}) estimated from the ankle and knee joint angles (SOL: Rack & Westbury 1969; MG: Herzog *et al.* 1992), which gives a speed expressed in terms of optimal muscle length,

$$\bar{V}_i = \frac{V_i}{L_i^{\mathrm{opt}}}. \tag{2.1}$$

Then, the normalized speeds of shortening ($\%V_i^{\max}$) were calculated by dividing the standardized shortening speeds ($\bar{V}_i$) by the maximal shortening speeds standardized to L_i^{opt} (i.e. $\bar{V}_{\mathrm{SOL}}^{\max} = 2.4 L_{\mathrm{SOL}}^{\mathrm{opt}}$: Spector *et al.* 1980; Sandercock & Heckman 1997; $\bar{V}_{\mathrm{MG}}^{\max} = 2.1 L_{\mathrm{MG}}^{\mathrm{opt}}$: Spector *et al.* 1980),

$$\%V_i^{\max} = \frac{\bar{V}_i}{\bar{V}_i^{\max}} \times 100\%, \tag{2.2}$$

which then gives a value of the instantaneous speed of shortening in terms of the maximal speed of shortening.

2.5. Definition of jumping phases

Two primary phases of jumping were defined based on the hindlimb kinematics: the preparatory phase, defined from the lift-off of the forelimbs until first ankle extension, and the propulsive phase, defined from first ankle extension to the end of paw contact (figure 1). The propulsive phase was further divided into four phases (P1, P2, P3 and P4) based on the speed of SOL muscle-tendon shortening (figure 1*d*). P1 ranged from the beginning of the propulsive phase to the instant at which the SOL muscle-tendon shortening speed reached half of its maximal shortening speed as evaluated in force–velocity testing *in situ* (i.e. $V_{\mathrm{SOL}} = 50\% V_{\mathrm{SOL}}^{\max}$ in figure 1*d*), and P2 ended when the SOL muscle-tendon shortening speed reached the maximal *in situ* speed (i.e. $V_{\mathrm{SOL}} = 100\% V_{\mathrm{SOL}}^{\max}$ in figure 1*d*). P3 ended at the instant of the actual peak shortening speed during the propulsive phase (note that the peak shortening speed during jumping may exceed the maximal *in situ* shortening speed) and, finally, P4 ended at the end of the propulsive phase. The RMS values of the full-wave rectified EMG activity were obtained for each phase (e.g. figure 1*e*,*f*, black filled circles connected by black lines). The average muscle forces and velocities for each phase were obtained by calculating mean values of these data for the separate propulsive phases.

2.6. Definition of deactivation phases

We observed two distinct deactivation phases for SOL EMG activity during the propulsive phase. The first typically happened around the late preparatory–early P1 phase (figure 1*f*, grey arrowhead); the second around peak SOL shortening speed, when the EMG amplitude reached baseline levels (figure 1*f*, black arrowhead). In order to define the onset of these deactivation phases, the average five-point-moving-average RMS curve of the normalized EMG activity relative to that for slow walking (see §2.8 for details) was calculated throughout the jump (figure 1*e*,*f*, dark grey line denoted by '5 point' in legend). A 'five-point-moving-average' was chosen to obtain a smooth linear envelope of the rectified EMG activity to define the deactivation points. This procedure was empirically derived such that deactivation points were not greatly affected by large single EMG bursts and still contained good temporal resolution (i.e. 2.5 ms). The first deactivation point (DA1) was defined as the first instant when the five-point-average RMS value became less than 30%, and no subsequent RMS value ever exceed 50% of its peak. The second deactivation point (DA2) was defined at the instant when the five-point-average EMG RMS values fell below three standard deviations of the baseline values (Neptune *et al.* 1997). The endpoints of MG EMG activity were defined in the same way as that for DA2. Finally, the RMS values of the full-wave rectified EMG activity between the onset of the preparatory phase and DA1, DA1 and DA2, and DA2 and the end of the propulsive phase were calculated.

In order to characterize the activation patterns around the initial preparatory phase, DA1, DA2 of the SOL and the endpoint of MG EMG activity, an ensemble average of the five-point-average EMG curves was obtained. First, the five-point-average of the normalized SOL EMG activity was divided into three phases: (i) the first 50 ms starting from the initial preparatory phase, (ii) between 25 ms before and 50 ms after DA1, and (iii) between 25 ms before and 17.5 ms after DA2. For the MG, the five-point-average curves were divided into two phases: (i) the first 50 ms starting from the initial preparatory phase and (ii) between 25 ms before and 17.5 ms after the endpoints of the MG EMG activity. Then, the RMS curves from all animals (35 trials) were averaged for each phase to obtain the ensemble average curves.

The time durations between the beginning of the propulsive phase and DA1 or DA2 or the onset of TA EMG activity were calculated as Δt_{DA1}, Δt_{DA2} and Δt_{TA}, respectively, and were divided by the entire time for the propulsive phase, Δt_{prop}, to calculate the first and second deactivation phase% (phase%$_{\mathrm{DA1}}$ and phase%$_{\mathrm{DA2}}$) and TA onset phase% (phase%$_{\mathrm{TA}}$), respectively.

2.7. Predictions of SOL force capacity

In order to investigate whether SOL forces were limited by contractile conditions, forces during the propulsive phase of jumping were predicted based on the muscle-tendon force–length, force–velocity and force–relaxation relationships. The force capacity based on the muscle-tendon force–length relationship was

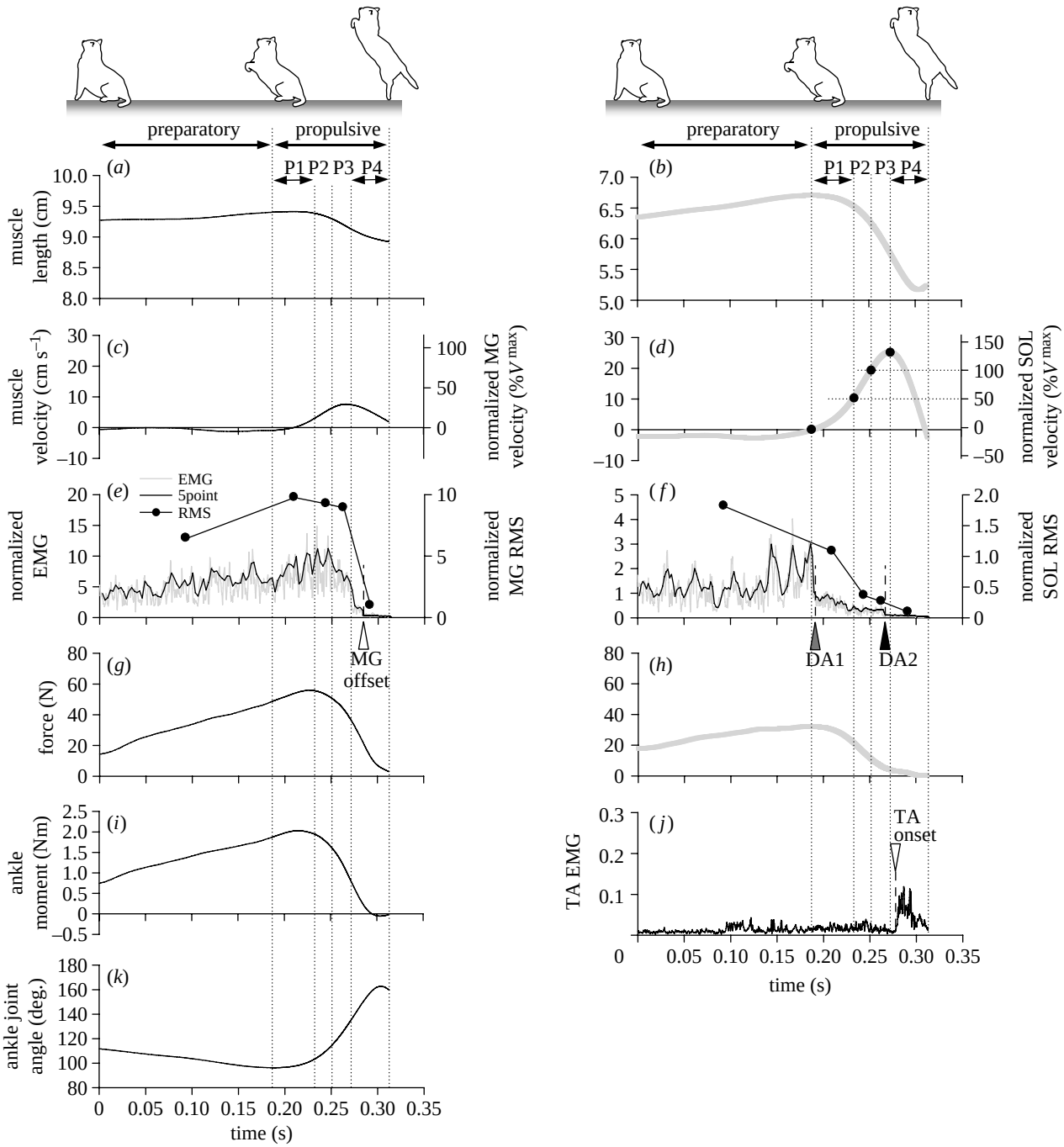

Figure 1. Example of time histories of (*a*) MG muscle-tendon length, (*b*) SOL muscle-tendon length, (*c*) MG muscle-tendon velocity, (*d*) SOL muscle-tendon velocity, (*e*) MG rectified EMG activity and corresponding average RMS value, (*f*) SOL rectified EMG activity and corresponding RMS value, (*g*) MG muscle force, (*h*) SOL muscle force, (*i*) resultant joint moment at the ankle, (*j*) TA rectified EMG activity and (*k*) ankle joint angle during the preparatory and propulsive phases of jumping. Muscle velocity was shown in both the absolute (left axis) and the normalized (right axis) values in (*c*,*d*). EMG and RMS values were normalized relative to those for level walking. The rectified EMG activities and the corresponding five-point-average curves were expressed in the left axis and the average RMS values for each jumping phase were expressed in the right axis in (*e*,*f*). Shortening velocity and extensor moment were defined as positive. The preparatory and propulsive phases were defined based on the cat hindlimb kinematics. The propulsive phase was further divided into four segments, P1–P4, defined based on the speeds of SOL shortening. The onsets of two distinct deactivation phases for SOL EMG activity, DA1 and DA2, are denoted by grey and black arrowheads in (*f*).

predicted by the force–length/ankle joint angle relationship for cat SOL with the ankle joint angle as input (Rack & Westbury 1969). The force capacity based on the muscle-tendon force–velocity relationship was estimated by using Hill's force–velocity equation for cat SOL with the standardized shortening speed relative to the optimal length as input (Spector *et al.* 1980). Finally, the force–relaxation relationship was estimated using the following equation, since SOL force in the latter part of jumping was influenced by SOL deactivation:

$$F_{\mathrm{relax}} = F_{\mathrm{init}}\left[\frac{(a_1+1)}{(a_1+e^{a_2 t})}\right], \qquad (2.3)$$

where F_{relax} and F_{init} are the predicted force potential and the experimentally observed force at the beginning of the propulsive phase, respectively, a_1 and a_2 are constants and t is the time from the beginning of the propulsive phase. To obtain constants a_1 and a_2, SOL force–relaxation data were fitted using equation (2.3) (see appendix A.2 for details). For predictions based on the force–length/velocity relationship, activation during the propulsive phase was assumed to remain at the same level as that at the beginning of the propulsive phase, so that the effects of muscle length and velocity on muscle force were tested independent of changes in activation. Force–relaxation curves were predicted for constant muscle length, so that relaxation was just a function of activation.

2.8. Statistical analysis

In order to compare EMG activity for jumping with that for slow walking (0.4 m s^{-1}), the EMG RMS values were normalized relative to the mean value between the onset and the offset of EMG activity for the stance phase of slow walking for each cat (Kaya *et al.* 2003). Mean EMG values for slow walking and jumping and mean values of EMG activity, muscle force, normalized shortening speed and joint moment for the different phases of jumping were compared across all animals using a repeated-measures analysis of variance (RM-ANOVA; SPSS Inc., Chicago, IL, USA). Coefficients of variation (CV = standard deviation/mean × 100%) were calculated for phase%$_{DA1}$, phase%$_{DA2}$ and phase%$_{TA}$ across all animals. The level of significance for all tests was $\alpha = 0.05$.

3. RESULTS

3.1. General results of jumping

MG and SOL were slightly stretched towards the end of the preparatory phase of jumping (figures 1*c*,*d* and 5, small negative velocity for both muscles), followed by a shortening during the propulsive phase. The shortening speed of both muscles progressively increased towards the end of P3 (figures 1*c*,*d* and 5), defined by the instant of peak SOL shortening speed (figure 1*d*). The absolute shortening speed of the SOL was consistently higher than that of the MG (figure 1*c*,*d*), since the shortening of the MG at the ankle was partly offset by MG stretching caused by knee extension.

The MG was activated to a similar extent for the preparatory and propulsive phases (figure 1*e*, filled circles; note that the RMS values were calculated as the average over each phase of jumping), while SOL EMG activity was high in the preparatory phase, but decreased continuously during the propulsive phase (figure 1*f*, filled circles). MG force gradually increased from the preparatory phase to P1, in concert with the ankle extensor moment curve (figure 1*g*,*i*), while the SOL force remained almost constant in the preparatory phase and the initial part of the propulsive phase. In the second half of the propulsive phase, SOL force decreased progressively and eventually reached a zero value prior to the end of the propulsive phase, when the required ankle extensor moment was still substantial (P4 phase, figure 1*h*,*i*). Thus, the shape of the MG force–time curve was similar to the ankle moment–time curve, while the SOL force–time curve was not (figure 1*g*–*i*).

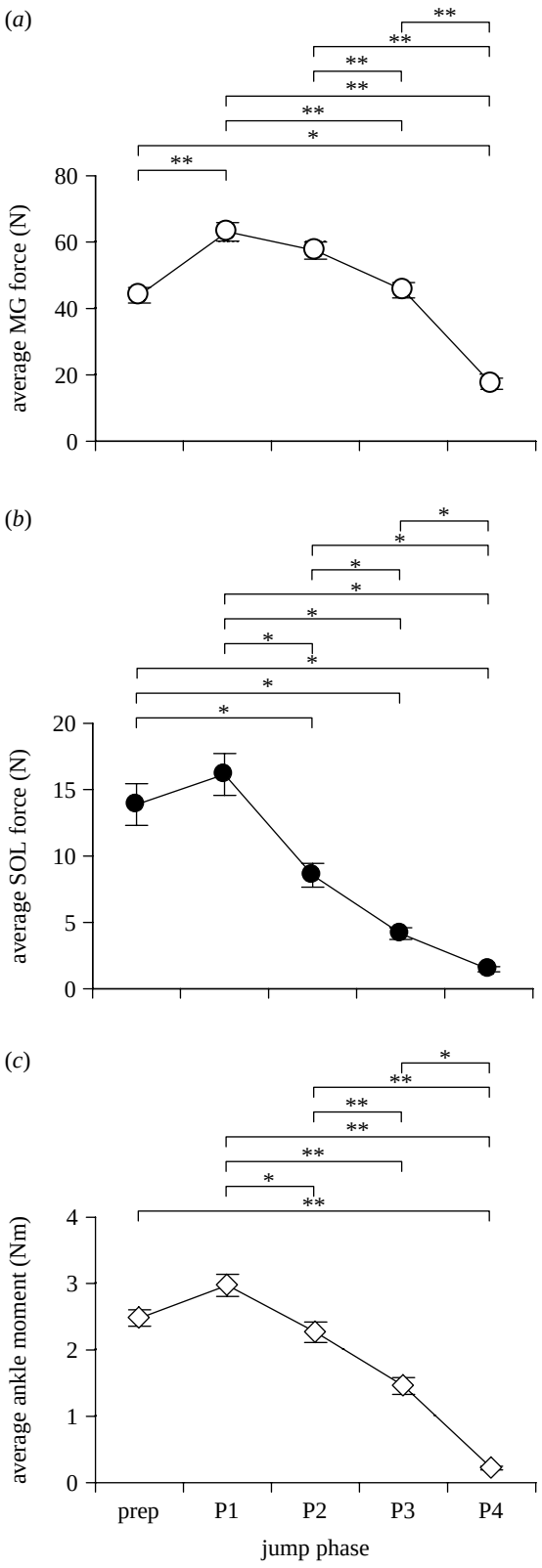

Figure 2. Means and standard errors of (*a*) the average MG force, (*b*) the SOL force and (*c*) the ankle moment for all animals during the preparatory (prep) and propulsive phases (P1–P4) of jumping. Significant differences between jumping phases are indicated by: $^{*}p < 0.05$; $^{**}p < 0.01$.

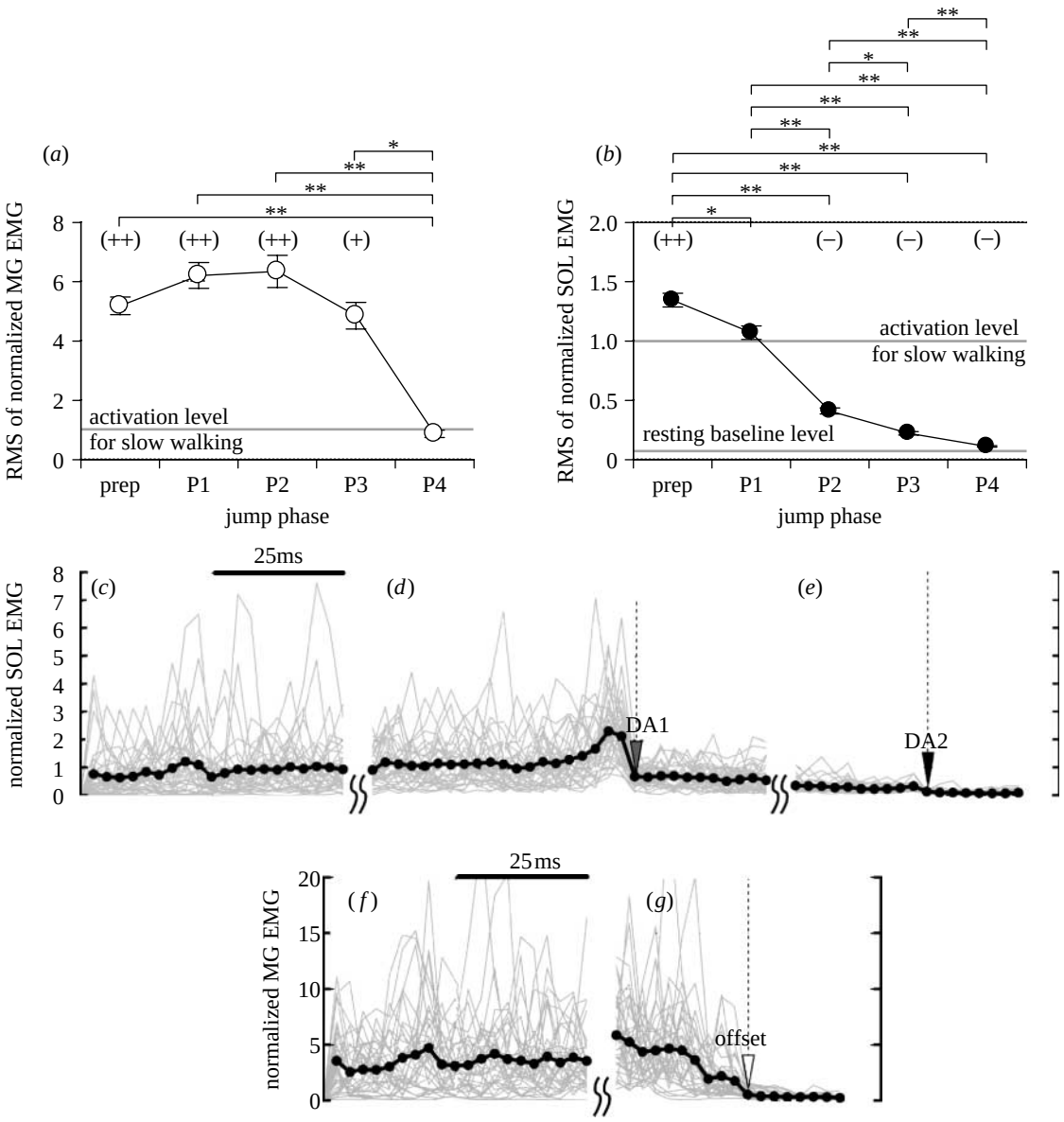

Figure 3. Means and standard errors of RMS values of normalized EMG activity for (*a*) MG and (*b*) SOL for all animals during each phase of jumping. Ensemble average RMS curves of normalized SOL EMG activity for (*c*) the first 25 ms starting from the beginning of the preparatory phase, (*d*) between 50 ms before and 25 ms after DA1 and (*e*) 25 ms before and 17.5 ms after DA2. Ensemble average RMS curves of normalized MG EMG activity for (*f*) the first 25 ms starting from the beginning of the preparatory phase and (*g*) between 25 ms before and 17.5 ms after the end of MG EMG activity. Individual average five-point-average EMG curves from all animals (35 trials in grey lines) were ensemble averaged to obtain the mean curves (black lines). DA1 and DA2 of SOL EMG activity are denoted by the grey and black arrowheads, respectively, and the end of EMG activity in the MG is denoted by the white arrowhead. Significant differences between jumping phases are indicated by: $^{*}p<0.05$; $^{**}p<0.01$. Significant differences between jumping phases and slow walking are indicated as follows: (+) $p<0.05$ greater than slow walking; (++) $p<0.01$ greater than slow walking; (−) $p<0.01$ smaller than slow walking.

3.2. MG/SOL force and ankle joint moment during jumping

Mean values of the average MG/SOL forces and average ankle moments across all animals were compared between the defined jump phases in figure 2. The average MG force increased from the preparatory phase to P1 and was maintained at a high level up to P3 (i.e. no significant decrease in MG force between the preparatory phase and P3 in figure 2*a*), while the average SOL force remained nearly constant from the preparatory phase to P1 (i.e. no significant increase in SOL force from the preparatory phase to P1 in figure 2*b*), and then decreased continuously towards negligibly small force (1.4 N) from P1 to P4 (figure 2*b*). The average ankle joint moments were extensor (positive) throughout the entire jump phase and remained high from the preparatory phase to P2 (figure 2*c*).

3.3. MG/SOL activation during jumping

Mean values of the normalized RMS values of MG/SOL EMG activity relative to those for slow walking across all animals were compared between the defined jumping phases in figure 3. The ensemble

average RMS curves of the normalized MG and SOL EMG activities across all animals are also shown in figure 3. Average MG EMG activity for the preparatory and the P1–P3 phases of jumping was five to seven times greater than that for slow walking (figure 3*a*,*f*,*g*). There was no difference in MG EMG activity from the preparatory phase to P3 (figure 3*a*), suggesting that the MG maintained high EMG activity levels throughout most of the jumping phases. Only MG EMG activity decreased towards the very end of the propulsive phase, when EMG activity levels became similar to those obtained for slow walking (P4, figure 3*a*). Average SOL EMG activity for the preparatory phase was 40% greater than that for level walking (figure 3*b*). During the propulsive phase, SOL EMG activity continuously decreased and was significantly lower for P2–P4 than that for slow level walking (figure 3*b*). SOL EMG activity during P4 was close to resting baseline values.

3.4. Deactivation of SOL during the propulsive phase of jumping

The continuous decrease in SOL EMG activity towards P4 (figure 3*b*) was mainly achieved by two distinct deactivation steps at points DA1 and DA2 (figure 3*d*,*e*). Mean values for normalized SOL EMG activity from the onset of the preparatory phase to DA1, from DA1 to DA2 (the first deactivation phase) and from DA2 to the end of the propulsive phase (the second deactivation phase) are shown in figure 4*a*. SOL EMG activity from the onset of the preparatory phase to DA1 (RMS = 1.4) was 40% greater than that for slow walking (RMS = 1). However, SOL EMG activity during the first deactivation phase (RMS = 0.6) was 40% lower than for slow walking and was close to the baseline levels for the second deactivation phase (figure 4*a*). Mean values of the normalized muscle-tendon velocity at DA1 and DA2 were 14% and 120% of $\bar{V}^{\max}_{\mathrm{SOL}}$, respectively (figure 4*b*), indicating that the DA1 and DA2 were triggered in P1 and P3, respectively.

3.5. MG/SOL muscle velocity during jumping

Mean values of the standardized and normalized MG/SOL muscle velocities for each jumping phase are shown separately in figure 5*a*,*b*. MG and SOL shortening speeds (positive values) continuously increased from the start of the preparatory phase to P3. The SOL shortening speeds for the P1–P4 phases were significantly higher than the corresponding MG shortening speeds (figure 5*a*,*b*). The peak MG shortening speed was $0.6L^{\mathrm{opt}}_{\mathrm{MG}}$ on average for P3 (figure 5*a*), which corresponds to only 30% of the maximal shortening speed for the MG (figure 5*b*). In contrast, the peak SOL shortening speed was $2.5L^{\mathrm{opt}}_{\mathrm{SOL}}$ on average for P3 (figure 5*a*) and exceeded the maximal *in situ* shortening speed ($105\%V^{\max}_{\mathrm{SOL}}$ in figure 5*b*).

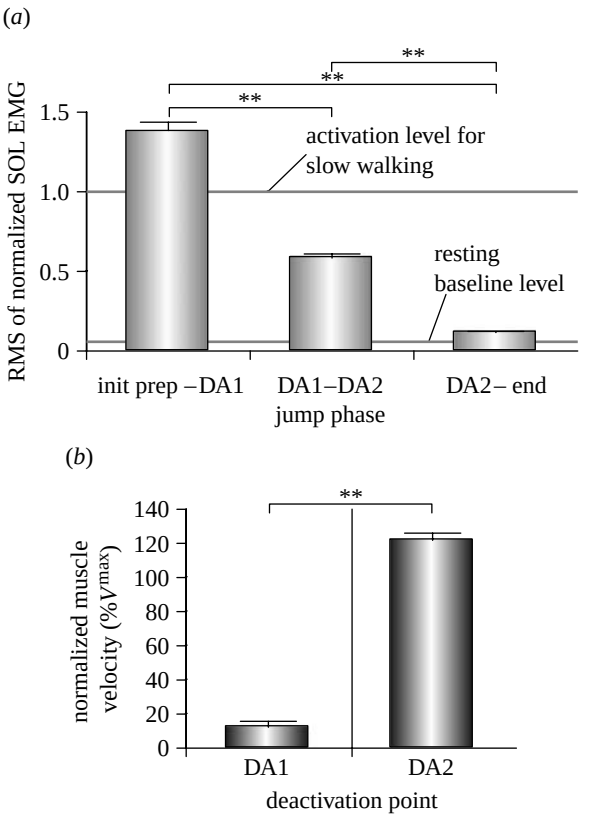

Figure 4. (*a*) Means and standard errors of RMS values of normalized SOL EMG activity from the initial preparatory phase to DA1 (init prep–DA1), from DA1 to DA2 (the first deactivation phase, DA1–DA2) and from DA2 to the end of propulsive phase (the second deactivation phase, DA2–end). (*b*) Means and standard errors of normalized SOL shortening speed for all animals at the onset of first (DA1) and second deactivations (DA2). Significant differences between the two conditions are indicated by: $^{**}p<0.01$.

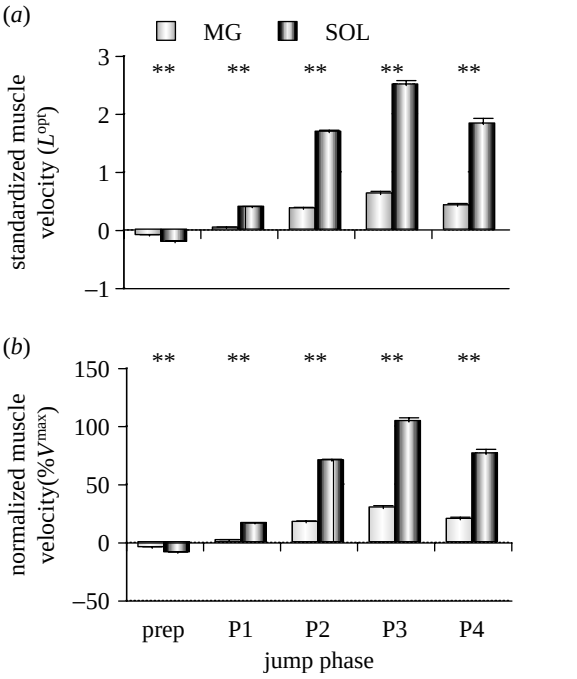

Figure 5. Means and standard errors of the (*a*) standardized and (*b*) normalized muscle velocities for MG and SOL for all animals during each phase of jumping. Significant differences between MG and SOL are indicated by: $^{**}p<0.01$.

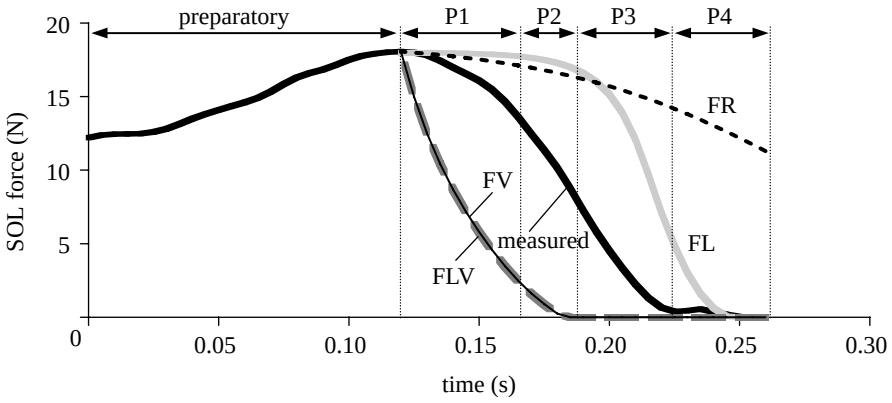

Figure 6. Example of time histories of measured SOL force (bold black line, 'measured') compared with predicted forces based on the force–length (grey line, 'FL'), the force–velocity (thin black line, 'FV'), the force–length–velocity (thick grey dashed line, 'FLV') and the force–relaxation relationship (dashed line, 'FR') during jumping. Note that the 'FV' and 'FLV' curves were virtually identical, since the force–velocity relationship dominates the force–length–velocity relationships during jumping.

4. DISCUSSION

Force-sharing between the cat MG and SOL has been shown to change dramatically for different speeds and intensities of locomotion and other movements, such as jumping and paw shaking. Forces and EMG activity of the MG seem to be in parallel with the ankle extensor moment requirements. For example, for increasing speeds/intensities of walking, ankle extensor moments increase, and so does MG force and EMG activity (Kaya *et al.* 2003). In contrast to this intuitively expected behaviour for ankle extensor muscle, the behaviour of the SOL is neither nearly as obvious, nor are observations about its behaviour consistent. For walking across a wide range of speeds, peak SOL forces have been found to be nearly constant (Walmsley *et al.* 1978; Hodgson 1983; Kaya *et al.* 2003), and SOL EMG activity has been said to remain constant (Walmsley *et al.* 1978; Hodgson 1983) or increase (Kaya *et al.* 2003; Gregor *et al.* 2006). However, for paw shaking, SOL forces and EMG activity are typically reported to be small or zero, because the movement is too fast for the SOL to contribute to the force production (Smith *et al.* 1980; Abraham & Loeb 1985*a*; Fowler *et al.* 1988). Thus, there seems to be a point when the SOL is deactivated in situations when an ankle extensor moment is required but its contractile conditions go beyond the SOL's capacity for force production. The question that arises from these findings is: are there situations in which SOL activation switches from a predominant excitatory to a predominant inhibitory state despite ankle extensor moment requirements?

During jumping, the MG and SOL go through contractile conditions ranging from isometric contractions at near-optimal lengths (preparatory phase) to high-speed shortening contractions at very short muscle lengths. Thus, we hypothesized that, for these quickly changing contractile conditions, force-sharing between the MG and SOL might change dramatically because the MG might function to satisfy the required ankle extensor moment throughout the jumping phase, while the SOL might be deactivated during the highly dynamic part of the jump through pre-programmed neural inputs by a central pattern generator or inhibitory pathways, as suggested (although not observed) for cat locomotion (Hodgson 1983; Nichols 1999).

4.1. Premature SOL deactivation during jumping

The SOL appears to be deactivated 'prematurely' in the propulsive phase of jumping, despite substantial ankle extensor moment requirements. This idea is illustrated by the decrease in SOL EMG activity and force in P2 compared with the preparatory–P1 phase (figures 2*b* and 3*b*).

In P2, the SOL approached its maximal shortening speed (100% $V_{\mathrm{SOL}}^{\max}$ in figure 1*d*), and its force capacity was approximately 0–15% of the maximal isometric force according to the force–velocity relationship (Spector *et al.* 1980). Moreover, SOL force (black bold line, figure 6) dropped much more quickly than predicted based on the force–length (grey line, figure 6) or force–relaxation relationship (dashed line, figure 6). Therefore, SOL force does not seem to be limited by length and activation, but by its force–velocity properties. Note that force decreases faster according to the force–velocity relationship than observed during jumping (figure 6). This result is probably caused by the way the force–velocity relationship was obtained, i.e. as the steady-state force at a given constant shortening speed, while the experimental force curve reflects the dynamic properties of the SOL, i.e. the elongation in tendons and aponeuroses delays the fascicle shortening speed (Gregor *et al.* 1988).

In P3, SOL shortening speed increased beyond its maximal speed of shortening (figures 1*f* and 5*b*). These high speeds of shortening are probably caused by the shortening of the remaining plantar flexor muscles (MG, lateral gastrocnemius and plantaris), which can generate much higher forces and contract relatively slower than the SOL for a given speed of ankle plantar flexion, owing to their primarily fast-twitch-fibred composition and biarticular arrangement. In this phase, EMG activity levels approached resting values (figure 3*b*). Thus, it appears that the SOL is prematurely deactivated in P2 and P3, when SOL force becomes severely limited by shortening speed.

In contrast to the SOL, MG EMG activity remained high until P3 (figure 3*a*). Furthermore, MG force at the beginning of the propulsive phase (figure 2*a*) was considerably smaller than its maximal isometric force (approx. 100 N, Spector *et al.* 1980), suggesting that the MG was not fully activated at that instant. Also, MG shortening speeds were always smaller than those for SOL, and the peak speed was not close to the maximal shortening speed for cat MG (30% V_{MG}^{max}, figure 5*b*). This is due to the two-joint nature of the MG, where shortening at the ankle is partly offset by stretching at the knee during jumping. Therefore, MG force was not nearly as limited by the speed of shortening as SOL force, and increases in activation caused increases in MG force.

4.2. Functional implication of 'premature' SOL deactivation

The results of this study suggest that the rapid ankle extension during P2–P3 caused SOL shortening speeds to exceed the maximal *in situ* shortening speed. Therefore, the SOL would not be able to produce much force and work (if any) even if it was fully activated. It appears that the neuromuscular system detects when SOL activation does not produce force, but activation would cost energy. Therefore, deactivation of the SOL appears to be a clever way to save energy in situations in which ankle moments would profit from SOL activation, but the contractile conditions do not allow for force and work production.

4.3. Potential neural pathways for SOL deactivation

Premature deactivation of the SOL in P2 and P3 appears to occur in two distinct phases (figures 1*f* and 3*d*,*e*). SOL shortening speeds at the onset of these deactivation phases (DA1 and DA2) were 14% and 120% of the maximal shortening speed, respectively (figure 4*b*), suggesting that the first deactivation occurs as the SOL passes from an isometric to a shortening state, and the second occurs when SOL shortening speed reaches its absolute maximum value.

In order to discuss the EMG–force relationship of a muscle, the electromechanical delay (EMD) must be considered. The EMD between the offset of SOL EMG activity and that of force is approximately 100–120 ms (Guimaraes *et al.* 1995). The time interval between the beginning of the propulsive phase (thus, beginning of SOL shortening) and the instant of peak SOL shortening speed was 112 ms on average (column 'all', figure 7). Hence, one might speculate that the first deactivation step was evoked around the initial propulsive phase to avoid an excessive amount of muscle activation when the SOL force potential is severely limited by its high shortening speed. One might further hypothesize that the first deactivation is caused by spindle-related speed-dependent pathways, since the first deactivation was typically associated with the beginning of muscle shortening in early P1 (figures 1 and 4*b*). Such inhibitory effects caused by the decrease in firing rate of group Ia spindles have been observed in the E3 phase of cat locomotion which is

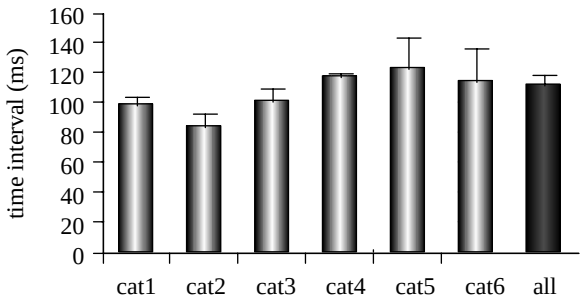

Figure 7. Means and standard errors of the time interval between the beginning of the propulsive phase and the instant of peak SOL shortening speed.

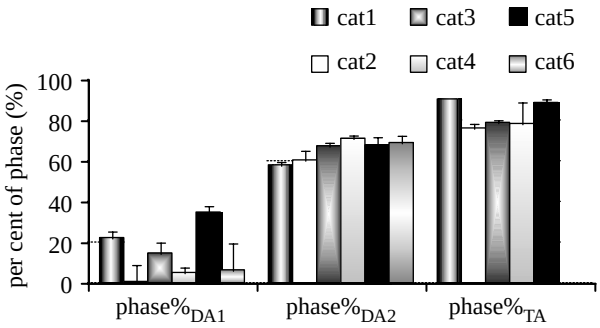

Figure 8. Means and standard errors of the time duration as the percentage of the time duration for the propulsive phase from the onset of the propulsive phase to DA1 (phase%$_{DA1}$), DA2 (phase%$_{DA2}$) and the onset of TA EMG (phase%$_{TA}$) for each animal. Note that TA EMG activity for cat6 was not measured.

associated with active soleus shortening (Prochazka *et al.* 1989). In addition to that one might speculate that centrally driven neural inputs also contribute to this deactivation, since the first deactivation occurs abruptly, while the preceding SOL shortening is gradually changing and is relatively slow.

The coefficient of variation for the second deactivation phase (phase%$_{DA2}$) was small (16%) compared with the first deactivation phase (phase%$_{DA1}$; 119%), suggesting that the second deactivation might be tightly related to the particular phase of jumping (figure 8) and, therefore, might be a pre-programmed phase-dependent event that is triggered by the central pattern generator.

Reciprocal inhibition from antagonistic ankle flexor muscles, such as the TA, also might cause SOL deactivation during the propulsive phase of jumping. However, the TA was activated only at the end of the propulsive phase (phase%$_{TA}$=80–90%, figure 8), while SOL deactivation occurred earlier in the propulsive phase (phase%$_{DA2}$=60–70%, figure 8). Therefore, premature deactivation of the SOL is probably not caused by reciprocal inhibition from the active antagonistic TA. In principle, such an inhibition is possible from the inactive TA prior to SOL active shortening; however, this possibility cannot be evaluated from our results.

It has been suggested that the SOL receives inhibitory signals from cutaneous (Burke *et al.* 1970; Kanda *et al.* 1977; Abraham & Loeb 1985*b*) and

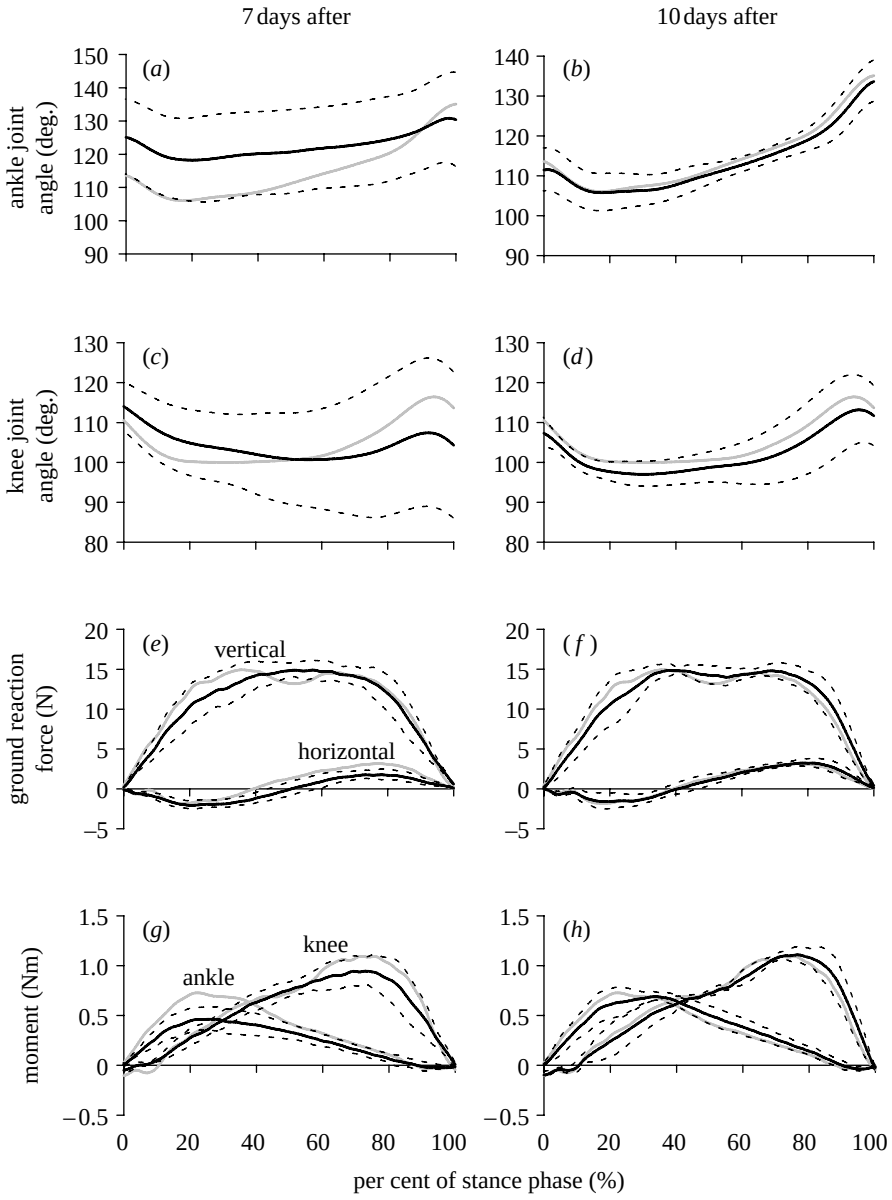

Figure 9. Comparison of (*a*,*b*) ankle, (*c*,*d*) knee joint angles, (*e*,*f*) horizontal and vertical ground reaction forces, and (*g*,*h*) ankle and knee joint moments obtained (*a*,*c*,*e*,*g*) before and 7 days after surgery and (*b*,*d*,*f*,*h*) before and 10 days after surgery from a single animal. The mean curves obtained before surgery are shown by the grey lines, and those obtained after surgery are shown by the black lines with the corresponding standard deviations (dashed lines). On the horizontal axis, 0% corresponds to the instant of paw contact and 100% corresponds to the instant of paw off.

rubrospinal pathways (Burke *et al.* 1970), and these pathways have been associated with a speed-dependent SOL inhibition during locomotion (Hodgson 1983) and paw shaking (Smith *et al.* 1980, 1985). Since the ground reaction forces during jumping were greater than that for walking, cutaneous afferents from the paws might also play a role in SOL deactivation. The possible effects of rubrospinal pathways on SOL inhibition cannot be evaluated from the results of this study, and it will be challenging to evaluate the role of these pathways during voluntary movements.

In summary, we found that the MG and SOL contribute in very different ways to the ankle extensor moment in cat jumping. MG force and EMG activity patterns follow the ankle moment–time curve, while SOL force and EMG activity do not. Specifically, SOL EMG activity is stopped 'prematurely', causing SOL force to drop to virtually zero at a time when ankle extensor moments are still substantial and must be provided by agonists of the SOL. We propose tentatively that the first SOL deactivation might be caused by the decrease in group Ia firing associated with active shortening, and the second might be a pre-programmed response inherent to the central pattern generator.

5. CONCLUSION

Cat soleus is prematurely deactivated in the propulsive phase of jumping as shortening speeds approach maximal values. We conclude that the SOL is deactivated despite great ankle extensor requirements to save energy as force and work output would be small or zero, and thus the metabolic cost per unit of work would become extensive. We propose that, in general,

neuromuscular pathways are equipped to detect when muscle work is severely compromised by a muscle's contractile conditions, and thus there exist inhibitory pathways that prevent costly muscle activation in these situations.

All surgical procedures were performed according to the guidelines of the Canadian Council on Animal Care and were approved by the Life Sciences Animal Ethics Committee of the University of Calgary.

The authors would like to thank Dr T.R. Nichols for his comments and suggestions on this manuscript and are also grateful to Hoa Nguyen and Andrzej Stano for their technical support. This work was supported by the Alberta Heritage Foundation for Medical Research, NSERC of Canada and the Olympic Oval Endowment Fund, University of Calgary.

APPENDIX A

A.1. Assessment of recovery from surgery

In figure 9, the ankle and knee joint angles, horizontal and vertical ground reaction forces, and the resultant ankle and knee joint moments from a single animal during the stance phase of slow walking obtained before and 7 days after surgery (figure 9*a*,*c*,*e*,*g*) or before and 10 days after surgery (figure 9*b*,*d*,*f*,*h*) were compared. The mean curves obtained before surgery are shown by the grey lines, and the mean curves 7 and 10 days after surgery are shown by the black lines. The amount of ankle and knee extension at 10 days after surgery indicated a greater and more complete recovery than those obtained 7 days after surgery (figure 9*a*–*d*). Specifically, the posterior (positive) horizontal ground reaction forces in the second half of stance and ankle and knee extensor (positive) moments 10 days after surgery were greater than those 7 days after surgery (figure 9*e*–*h*). Also, the ankle and knee joint angle curves obtained at 7 days post surgery were more variable (figure 9*a*,*c*) than those obtained at 10 days post surgery. Thus, for this animal, measurements obtained at 7 days post surgery were not considered for analysis while those at 10 days post surgery were.

A.2. Force–relaxation curve

The force potential for the activated SOL is typically predicted based on the force–length–velocity–activation relationships. However, for the second half of jumping, the SOL was deactivated, and therefore the SOL force was influenced by its force–relaxation property during that particular phase. Hence, in order to obtain the force–relaxation relationship, the *in situ* maximum isometric forces of cat SOL were measured at different muscle lengths (Herzog *et al.* 1992). Relaxation of the SOL was then quantified by the decay of force from its peak value until it fell below 1% of the peak force after deactivation. Force–relaxation curves from nine trials were normalized to the individual peak force values (which depend on muscle length) and then fitted by equation (2.3) in figure 10. Since the maximum isometric forces depend on the isometric lengths, the force values were normalized relative to the individual peak forces. Thus here, the maximum isometric force at each length, F_{init}, was set to 1. (Note that the maximum isometric force, F_{init}, during jumping was taken as the SOL force at the beginning of the propulsive phase in figure 6.) The normalized force–relaxation curves were consistent across muscle lengths (grey lines in figure 10), and, thus, the fitting curve was appropriate to represent the general characteristics of the force–relaxation curve for all muscle lengths (black line in figure 10).

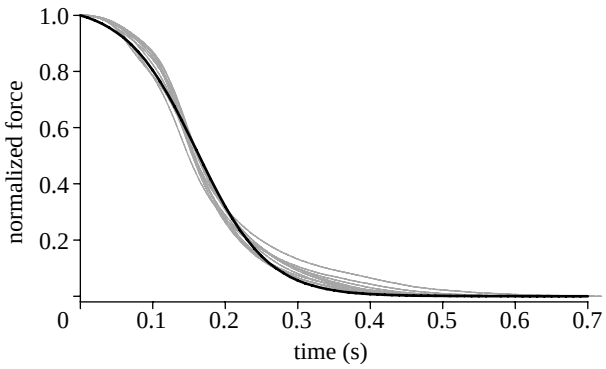

Figure 10. Force–relaxation curve of *in situ* isometric cat SOL force at different lengths. The curves from nine trials (grey lines) spanning the normal range of SOL motion were approximated with a best-fit curve (black line). The force values were normalized relative to the individual peak force values. The curves were fitted by $F_{\mathrm{relax}} = F_{\mathrm{init}}[(a_1+1)/(a_1+e^{a_2 t})]$, where F_{relax} and F_{init} are the predicted relaxation force and the force at the beginning of the relaxation phase ($F_{\mathrm{init}}=1$), respectively, a_1 and a_2 are fitting parameters and t is the time from the beginning of the relaxation phase. Fitting results: $a_1=26.7$, $a_2=20.5$.

REFERENCES

Abraham, L. D. & Loeb, G. E. 1985*a* The distal hindlimb musculature of the cat (patterns of normal use). *Exp. Brain Res.* **58**, 580–593.

Abraham, L. D. & Loeb, G. E. 1985*b* The distal hindlimb musculature of the cat. Cutaneous reflexes during locomotion. *Exp. Brain Res.* **58**, 594–603.

Andrews, J. G. 1995 Euler's and Lagrange's equations for linked rigid-body models of three-dimensional human motion. In *Three-dimensional analysis of human movement* (eds P. Allard, I. A. F. Stokes & J. P. Blanchi), pp. 145–175. Champaign, IL: Human Kinetics.

Ariano, M. A., Armstrong, R. B. & Edgerton, V. R. 1973 Hindlimb muscle fiber populations of five mammals. *J. Histochem. Cytochem.* **21**, 51–55.

Burke, R. E., Ten Bruggencate, G. & Jankowska, E. 1970 A comparison of peripheral and rubrospinal input to slow and fast motor units of triceps surae. *J. Physiol.* **207**, 709–732.

Fowler, E. G., Gregor, R. J. & Roy, R. R. 1988 Differential kinetics of fast and slow ankle extensors during the paw-shake in the cat. *Exp. Neurol.* **99**, 219–224. (doi:10.1016/0014-4886(88)90141-0)

Gregor, R. J., Roy, R. R., Whiting, W. C., Lovely, R. G., Hodgson, J. A. & Edgerton, V. R. 1988 Mechanical output of the cat soleus during treadmill locomotion: *in vivo* vs *in situ* characteristics. *J. Biomech.* **21**, 721–732. (doi:10.1016/0021-9290(88)90281-3)

Gregor, R. J., Smith, J. L., Smith, D. W., Oliver, A. & Prilutsky, B. I. 2001 Hindlimb kinetics and neural control

during slope walking in the cat: unexpected findings. *J. Appl. Biomech.* **17**, 277–286.

Gregor, R. J., Smith, D. W. & Prilutsky, B. I. 2006 Mechanics of slope walking in the cat: quantification of muscle load, length change, and ankle extensor EMG patterns. *J. Neurophysiol.* **95**, 1397–1409. (doi:10.1152/jn.01300.2004)

Grieve, D. W., Pheasant, S. & Cavanagh, P. R. 1978 Prediction of gastrocnemius length from knee and ankle joint posture. In *Biomechanics VI-A* (eds E. Asmussen & K. Jorgensen), pp. 405–418. Baltimore, MD: University Park Press.

Guimaraes, A. C., Herzog, W., Allinger, T. L. & Zhang, Y. T. 1995 The EMG-force relationship of the cat soleus muscle and its association with contractile conditions during locomotion. *J. Exp. Biol.* **198**, 975–987.

Herzog, W., Leonard, T. R., Renaud, J. M., Wallace, J., Chaki, G. & Bornemisza, S. 1992 Forces-length properties and functional demands of cat gastrocnemius, soleus, and plantaris muscles. *J. Biomech.* **25**, 1329–1335. (doi:10.1016/0021-9290(92)90288-C)

Herzog, W., Leonard, T. R. & Guimaraes, A. C. S. 1993 Forces in gastrocnemius, soleus, and plantaris tendons of the freely moving cat. *J. Biomech.* **26**, 945–953. (doi:10.1016/0021-9290(93)90056-K)

Hill, A. V. 1938 The heat of shortening and the dynamic constrants of muscle. *Proc. R. Soc. B* **126**, 136–195. (doi:10.1098/rspb.1938.0050)

Hodgson, J. A. 1983 The relationship between soleus and gastrocnemius muscle activity in conscious cats—a model for motor unit recruitment? *J. Physiol.* **337**, 553–562.

Hoy, M. G. & Zernicke, R. F. 1985 Modulation of limb dynamics in the swing phase of locomotion. *J. Biomech.* **18**, 49–60. (doi:10.1016/0021-9290(85)90044-2)

Kanda, K., Burke, R. E. & Walmsley, B. 1977 Differential control of fast and slow twitch motor units in the decerebrate cat. *Exp. Brain Res.* **29**, 57–74. (doi:10.1007/BF00236875)

Kaya, M., Leonard, T. & Herzog, W. 2003 Coordination of medial gastrocnemius and soleus forces during cat locomotion. *J. Exp. Biol.* **206**, 3645–3655. (doi:10.1242/jeb.00544)

Neptune, R. R., Kautz, S. A. & Hull, M. L. 1997 The effect of pedaling rate on coordination in cycling. *J. Biomech.* **30**, 1051–1058. (doi:10.1016/S0021-9290(97)00071-7)

Nichols, T. R. 1999 Receptor mechanisms underlying heterogenic reflexes among the triceps surae muscles of the cat. *J. Neurophysiol.* **81**, 467–478.

Prochazka, A., Trend, P., Hulliger, M. & Vincent, S. 1989 Ensemble proprioceptive activity in the cat step cycle: towards a representative look-up chart. *Prog. Brain. Res.* **80**, 61–74.

Rack, P. M. & Westbury, D. R. 1969 The effects of length and stimulus rate on tension in the isometric cat soleus muscle. *J. Physiol.* **204**, 443–460.

Sacks, R. D. & Roy, R. R. 1982 Architecture of the hind limb muscle of cats: functional significance. *J. Morph.* **173**, 185–195. (doi:10.1002/jmor.1051730206)

Sandercock, T. G. & Heckman, C. J. 1997 Force from cat soleus muscle during imposed locomotor-like movements: experimental data versus Hill-type model predictions. *J. Neurophysiol.* **77**, 1538–1552.

Smith, J. L., Edgerton, V. R., Betts, B. & Collatos, T. C. 1977 EMG of slow and fast ankle extensors of cat during posture, locomotion, and jumping. *J. Neurophysiol.* **40**, 503–513.

Smith, J. L., Betts, B., Edgerton, V. R. & Zernicke, R. F. 1980 Rapid ankle extension during paw shakes: selective recruitment of fast ankle extensors. *J. Neurophysiol.* **43**, 612–620.

Smith, J. L., Hoy, M. G., Koshland, G. F., Phillips, D. M. & Zernicke, R. F. 1985 Intralimb coordination of the paw-shake response: a novel mixed synergy. *J. Neurophysiol.* **54**, 1271–1281.

Spector, S. A., Gardiner, P. F., Zernicke, R. F., Roy, R. R. & Edgerton, V. R. 1980 Muscle architecture and force–velocity characteristics of cat soleus and medial gastrocnemius: implications for motor control. *J. Neurophysiol.* **44**, 951–960.

Walmsley, B., Hodgson, J. A. & Burke, R. E. 1978 Forces produced by medial gastrocnemius and soleus muscles during locomotion in freely moving cats. *J. Neurophysiol.* **41**, 1203–1216.

Woltring, H. J. 1986 A FORTRAN package for generalized, cross-validatory spline smoothing and differentiation. *Adv. Eng. Softw.* **8**, 104–113.

Zajac, F. E. 1985 Thigh muscle activity during maximum-height jumps by cats. *J. Neurophysiol.* **53**, 979–994.